Electronic Supplementary Material (ESI) for CrystEngComm.
This journal is © The Royal Society of Chemistry 2020

Supplementary Materials

The influence of structure on the neutron scattering properties of the polymorphic complexes: 6,6'-dimethyl-2,2'-dipyridyl with halo derivatives of benzoquinone acids

Magdalena Rok[a], Marcin Moskwa[a], Przemysław Dopieralski[a], Wojciech Medycki[b], Michaela Zamponi[c], Grażyna Bator[a]

[a]Faculty of Chemistry, University of Wroclaw, 14 F. Joliot – Curie, 50-383 Wroclaw, Poland

[b]Institute of Molecular Physics, Polish Academy of Sciences, Smoluchowskiego 17, 60-179 Poznań, Poland

[c] Forschungszentrum Jülich GmbH, Jülich Centre for Neutron Science (JCNS) at Heinz Maier-Leibnitz Zentrum (MLZ), Lichtenbergstr. 1, 85748 Garching, Germany

*e-mail: magdalena.rok@chem.uni.wroc.pl

CAPTIONS OF FIGURES

CAPTION OF TABLES

THEORETICAL PARTS

a) α-66DMBP·CLA

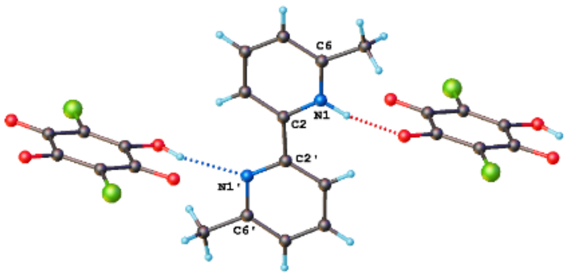

b) β-66DMBP·CLA

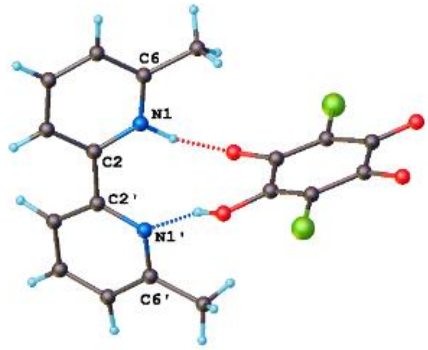

Fig. S1. The formation of the alternating acid and base molecules through hydrogen bonding (dotted lines) a) on two sides of molecule (α-form); b) on one side of the molecule (β-form).

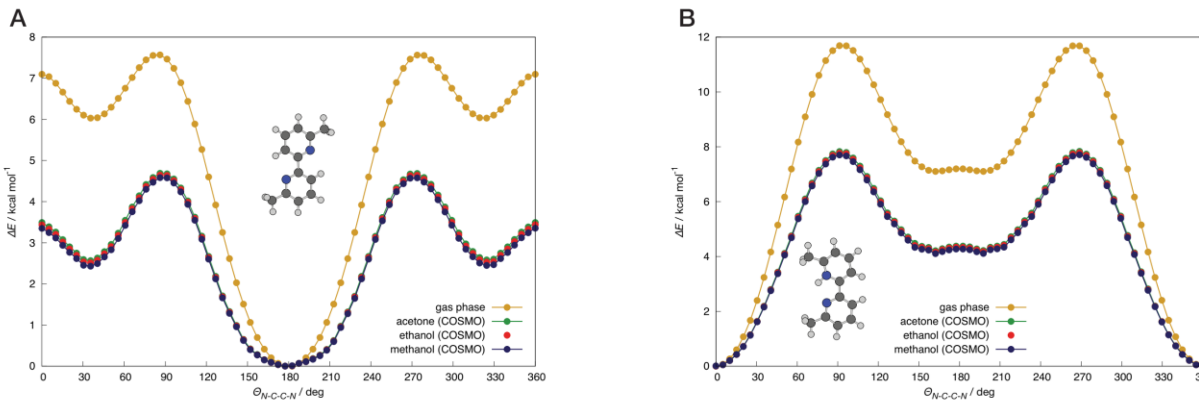

Fig. S2. Energy profiles along the dihedral angle N-C-C-N for the 6,6'-dimethyl-2,2'-bipyridinium (panel A) and N-protonated 6,6'-dimethyl-2,2'-bipyridinium cation (panel B) for the T = 0K case obtained by ORCA 3.0.3 with B3LYP/G/cc-pVTZ. Molecules are shown in insets Θ = 180° and Θ = 0° respectively). Gold points represent an isolated molecule and green, red and blue points (curves) results from Conductor--like Screening Model (COSMO) for acetone, ethanol and methanol, respectively.

We performed conformational analysis on the 6,6'-dimethyl-2,2'-bipyridinium and its cation protonated on the one of the nitrogen atoms by means of the static and dynamic simulations. In a static approach we used two different programs and continuous models: firstly the Polarizable Continuum Model (PCM) [1,2] with the integral equation formalism variant (IEFPCM [3-6] as implemented in GAUSSIAN [7] software and secondly the Conductor Like Screening Model (COSMO) [8] as implemented in ORCA [9] software. For review see [10]. The preliminary optimization of the geometrical structures and harmonic vibrational analysis have been performed using the GAUSSIAN [7] and ORCA [9] softwares. Our method of choice was DFT--B3LYP and B3LYP/G as implemented in GAUSSIAN and ORCA, respectively (to ensure consistency between static calculations), with the cc-pVTZ basis set [11]. The minima on the potential energy surface (PES) have been confirmed by the analysis of the harmonic vibrational frequencies. All static calculations were performed for the isolated molecules and with dielectric constants for three selected solvents i.e. acetone, ethanol and methanol. Energy scans for $\Theta_{NCCN} = 180^o$ were performed with $\Delta\Theta = 5^o$. In order to acquire more accurate results in terms of solvent effects we performed the *ab initio* molecular dynamics calculations [12] using the efficient Car—Parrinello [13] propagation scheme as implemented in the *CPMD* program package version 3.17.3 [14]. We took into consideration, similarly as in static approach, either not protonated or N-protonated molecule but in order to reduce cost of computations we considered only acetone and methanol solutions. Simulations were carried out in the range of torsion angle at about $\Theta_{NCCN} = 0 - 180^o$. The molecule was placed in a cubic supercell of 15 Å in length together with 37 methanol molecules in the first simulation and 15 acetone molecules in second one (for both, not protonated and N--protonated 66DMBP) to properly subject a solvate molecule to periodic boundary conditions. CPMD simulation was performed using the B3LYP/cc-pVTZ optimized geometry as the starting point. Following the initial equilibration period (ca. 20 000 steps, 2 ps), where each degree of freedom had a separate Nose-Hoover-chain (NHC) thermostat [15], the data were collected over trajectories spanning 95 000 steps (ca. 9.2 ps) for every point on the curves. During the initial equilibration period, each atom was thermalized before the start of a proper run with only one, global NHC thermostat. A kinetic energy cutoff of 70 *Ry* was used for the electron plane-wave basis and Γ-point sampling of the Brillouin zone. The Troullier-Martins normconserving pseudopotentials [16], the Becke et al. (BLYP) exchange and correlation functional [17, 18] within the Kohn-Sham formalism and empirical van der Waals corrections by Grimme [19] were applied. The simulations were performed in the canonical ensemble at 295 K. To control the temperature of the system, the NHC thermostat was turned on (to control the kinetic energy of the nuclei as well as the fictitious energy of the orbitals) and set at a frequency of 3000 cm^{-1}. A molecular dynamics time step of $\Delta t = 4$ a.u. (ca. 0.097 fs) was used for the integration of the Car-Parrinello equations of motion using a fictitious mass parameter for the orbitals of 400 a.u. together with the proper atomic masses. The activation free energies as a function of torsion angle Θ_{NCCN} were evaluated by means of AIMD simulations [12] in the condensed phase at 295 K in conjunction with enhanced sampling technique *ab initio* thermodynamic integration-based constrained ('blue moon') [20,21] AIMD; see e.g. Ref. 12 for detailed methodological background information. The VMD [22] (Visualize Molecular Dynamics) program has been used for data visualization.

References:

[1] S. Miertus, E. Scrocco, J. Tomasi, Chemical Physics 1981, 55, 117 - 129.
[2] S. Miertus, J. Tomasi, Chemical Physics 1982, 65, 239 - 245.
[3] E. Cances, B. Mennucci, J. Tomasi, The Journal of Chemical Physics 1997,107, 3032 - 3041.
[4] B. Mennucci, J. Tomasi, The Journal of Chemical Physics 1997, 106, 5151 -5158.
[5] B. Mennucci, E. Cances, J. Tomasi, The Journal of Physical Chemistry B 1997, 101, 10506 - 10517.
[6] J. Tomasi, B. Mennucci, E. Cancs, Journal of Molecular Structure: THEOCHEM 1999, 464, 211 - 226.
[7] M. J. Frisch, G. W. Trucks, H. B. Schlegel, G. E. Scuseria, M. A. Robb, J. R. Cheeseman, G. Scalmani, V. Barone, B. Mennucci, G. A. Petersson, H. Nakatsuji, M. Caricato, X. Li, H. P. Hratchian, A. F. Izmaylov, J. Bloino, G. Zheng, J. L. Sonnenberg, M. Hada, M. Ehara, K. Toyota, R. Fukuda, J. Hasegawa, M. Ishida, T. Nakajima, Y. Honda, O. Kitao, H. Nakai, T. Vreven, J. A. Montgomery, J. E. Peralta, F. Ogliaro, M. Bearpark, J. J. Heyd, E. Brothers, K. N. Kudin, V. N. Staroverov, R. Kobayashi, J. Normand, K. Raghavachari, A. Rendell, J. C. Burant, S. S. Iyengar, J. Tomasi, M. Cossi, N. Rega, J. M. Millam, M. Klene, J. E. Knox, J. B. Cross, V. Bakken, C. Adamo, J. Jaramillo, R. Gomperts, R. E. Stratmann, O. Yazyev, A. J. Austin, R. Cammi, C. Pomelli, J. W. Ochterski, R. L. Martin, K. Morokuma, V. G. Zakrzewski, G. A. Voth, P. Salvador, J. J. Dannenberg, S. Dapprich, A. D. Daniels, Farkas, J. B. Foresman, J. V. Ortiz, J. Cioslowski, D. J. Fox, Gaussian 09, Revision D.01 , 2009 .
[8] S. Sinnecker, A. Rajendran, A. Klamt, M. Diedenhofen, F. Neese, J. Phys. Chem. A 2006, 110, 2235 - 2245.
[9] F. Neese, WIREs Comput. Mol. Sci. 2012, 2, 73 - 78.
[10] J. Tomasi, B. Mennucci, R. Cammi, Chemical Reviews 2005, 105, 2999 - 3094.
[11] J. T. H. Dunning, J. Chem. Phys. 1989, 90, 1007.
[12] D. Marx, J. Hutter, Ab Initio Molecular Dynamics: Basic Theory and Advanced Methods, Cambridge University Press, Cambridge, 2009.
[13] R. Car, M. Parrinello, Phys. Rev. Lett. 1985, 55, 2471 - 2474.
[14] J. Hutter, et al., CPMD Program Package, see http://www.cpmd.org.
[15] G. J. Martyna, M. L. Klein, M. Tuckerman, J. Chem. Phys. 1992, 97, 2635 - 2643.
[16] N. Troullier, J. L. Martins, Phys. Rev. B 1991, 43, 1993 - 2006.
[17] A. D. Becke, Phys. Rev. A 1988, 38, 3098 - 3100.
[18] C. Lee, W. Yang, R. G. Parr, Phys. Rev. B 1988, 37, 785 - 789.
[19] S. Grimme, J. Comp. Chem. 2006, 27, 1787.
[20] E. Carter, G. Ciccotti, J. Hynes, R. Karpal, Chem. Phys. Lett. 1989, 156, 472 - 476.
[21] M. Sprik, G. Ciccotti, J. Chem. Phys. 1998, 109, 7737 - 7744.
[22] W. Humphrey, A. Dalke, K. Schulten, J. Molec. Graphics 1996, 14, 33.

EXPERIMENTAL PARTS

a)

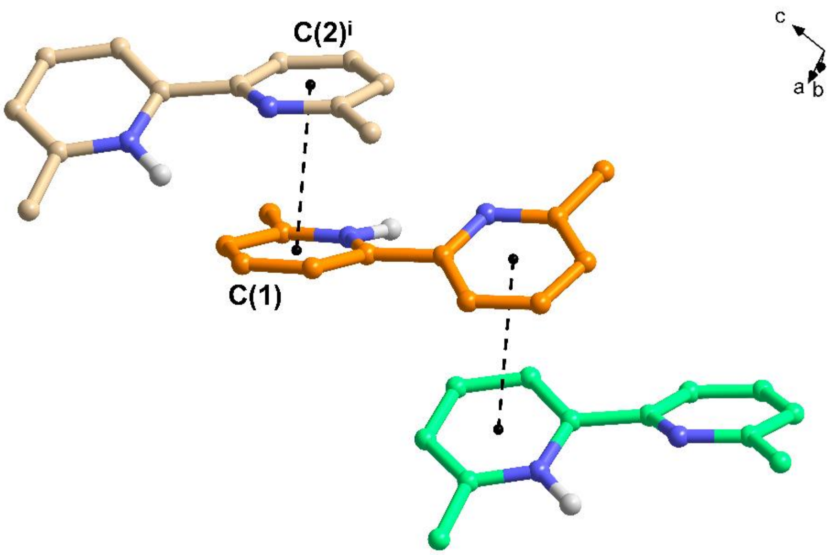

b)

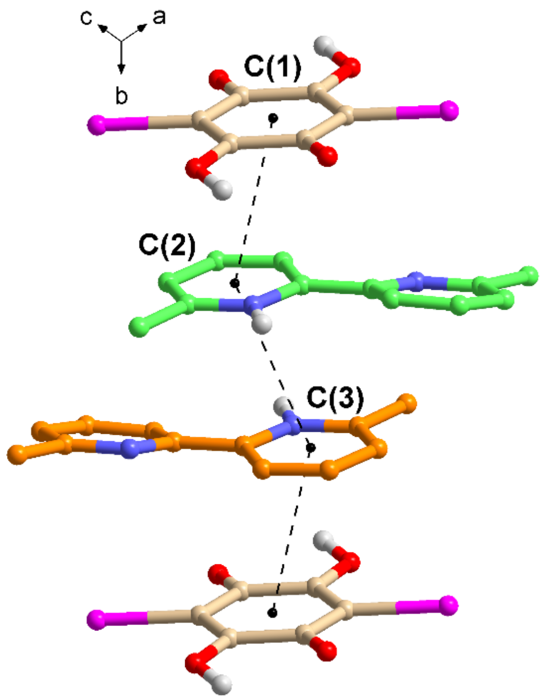

Fig. S3. C(X)···C(Y) contacts (black dashed lines) stabilizing the crystal structure of a) **1,** and b) **3**. C-bound H atoms have been omitted for clarity. Symmetry codes are listed in Table S5.

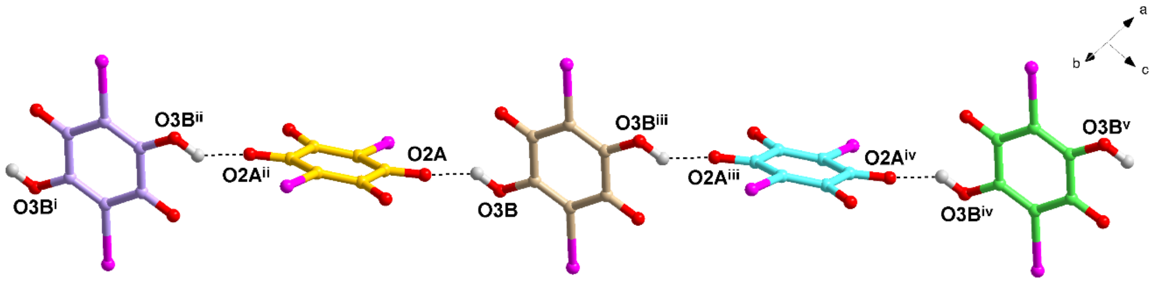

Fig. S4. The supramolecular chain of the **3** formed by O–H···O (black dashed lines) between dianion and neutral form of IA acid. Symmetry codes: (i) x−1, y, z−1; (ii) −x+1, −y+1, −z+1; (iii) −x+2, −y+1, −z+2; (iv) x+1, y, z+1; (v) −x+3, −y+1, −z+3.

Table S1. Crystal data and structure refinement parameters for **1, 2** and **3**.

Compound:	**1**	**2**	**3**
Crystal data			
Chemical formula	$C_{12}H_{13}N_2 \cdot C_6HBr_2O_4$	$C_{12}H_{13}N_2 \cdot 0.5(C_6Br_2O_4)$	$C_{12}H_{13}N_2 \cdot 0.5(C_6I_2O_4) \cdot 0.5(C_6H_2I_2O_4)$
M_r	482.13	333.18	576.11
Crystal system, space group	Monoclinic, $P2_1/c$	Triclinic, $P\bar{1}$	Triclinic, $P\bar{1}$
Temperature (K)	150(2)	100(2)	100(2)
a, b, c (Å)	15.252(4), 11.926(2), 10.272 (4)	7.792(4), 9.705(3), 9.938(5)	10.026(2), 10.281(2), 10.526(2)
α, β, γ (°)	90, 108.83(3), 90	94.41(4), 106.41(5), 110.28(3)	110.26(2), 92.56(2), 113.13(2)
V (Å^3)	1768(4)	663(2)	915(4)
Z	4	2	2
Radiation type	Mo $K\alpha$	Mo $K\alpha$	Mo $K\alpha$
μ (mm^{-1})	4.61	3.10	3.46
Crystal size (mm)	0.42 × 0.24 × 0.19	0.25 × 0.14 × 0.13	0.26 × 0.18 × 0.15
Data collection			
No. of measured, independent and observed [$I > 2\sigma(I)$] reflections	16895, 3297, 2826	3927, 2436, 2252	10778, 3402, 3239
R_{int}	0.096	0.021	0.023
$(\sin \theta/\lambda)_{max}$ (Å^{-1})	0.606	0.606	0.606
Refinement			
$R[F^2 > 2\sigma(F^2)]$, $wR(F^2)$, S	0.043, 0.116, 1.03	0.026, 0.056, 1.05	0.019, 0.054, 1.07
No. of reflections	3297	2436	3402
No. of parameters	243	186	237
$\Delta\rho_{max}$, $\Delta\rho_{min}$ (e Å^{-3})	0.90, -0.84	0.53, -0.37	0.83, -0.44

Table S2. Geometric parameters (Å, º) for 66DMBP·BRA **(1)**

Geometric parameters [Å, º] for **(1)**			
bond lengths [Å]			
Br1—C1	1.888(4)	C14—H14	0.9500
Br2—C4	1.890(3)	C15—C16	1.381(5)
C1—C2	1.348(5)	C15—H15	0.9500
C1—C6	1.459(5)	C16—C17	1.501(5)
C2—O2	1.327(4)	C17—H17A	0.9800
C2—C3	1.518(5)	C17—H17B	0.9800
O2—H2	0.99(4)	C17—H17C	0.9800
C3—O3	1.264(4)	N21—C26	1.344(5)
C3—C4	1.387(5)	N21—C22	1.354(5)
C4—C5	1.414(5)	C22—C23	1.388(5)
C5—O5	1.232(4)	C23—C24	1.377(6)
C5—C6	1.555(5)	C23—H23	0.9500
C6—O6	1.211(4)	C24—C25	1.384(6)
N11—C16	1.340(5)	C24—H24	0.9500
N11—C12	1.354(4)	C25—C26	1.390(6)
N11—H11	1.04(4)	C25—H25	0.9500
C12—C13	1.390(5)	C26—C27	1.512(5)
C12—C22	1.476(6)	C27—H27A	0.9800
C13—C14	1.387(6)	C27—H27B	0.9800
C13—H13	0.9500	C27—H27C	0.9800
C14—C15	1.388(6)		
angles [º]			
C6—C1—Br1	117.6(2)	N11—C16—C17	118.3(3)
O2—C2—C1	121.5(3)	C15—C16—C17	122.6(3)
O2—C2—C3	116.6(3)	C16—C17—H17A	109.5
C1—C2—C3	121.9(3)	C16—C17—H17B	109.5
C2—O2—H2	113(2)	H17A—C17—H17B	109.5
O3—C3—C4	126.3(3)	C16—C17—H17C	109.5
O3—C3—C2	115.8(3)	H17A—C17—H17C	109.5
C4—C3—C2	118.0(3)	H17B—C17—H17C	109.5
C3—C4—C5	123.6(3)	C26—N21—C22	118.7(3)
C3—C4—Br2	117.2(2)	N21—C22—C23	122.6(4)
C5—C4—Br2	119.1(2)	N21—C22—C12	116.9(3)
O5—C5—C4	125.7(3)	C23—C22—C12	120.4(3)
O5—C5—C6	116.9(3)	C24—C23—C22	118.2(4)
C4—C5—C6	117.3(3)	C24—C23—H23	120.9
O6—C6—C1	123.6(3)	C22—C23—H23	120.9
O6—C6—C5	118.7(3)	C23—C24—C25	119.7(4)

C1—C6—C5	117.8(3)	C23—C24—H24	120.2
C16—N11—C12	123.4(3)	C25—C24—H24	120.2
C16—N11—H11	118(2)	C24—C25—C26	119.4(4)
C12—N11—H11	118(2)	C24—C25—H25	120.3
N11—C12—C13	118.9(3)	C26—C25—H25	120.3
N11—C12—C22	116.9(3)	N21—C26—C25	121.3(3)
C13—C12—C22	124.1(3)	N21—C26—C27	116.5(3)
C14—C13—C12	118.8(3)	C25—C26—C27	122.1(4)
C14—C13—H13	120.6	C26—C27—H27A	109.5
C12—C13—H13	120.6	C26—C27—H27B	109.5
C13—C14—C15	120.5(4)	H27A—C27—H27B	109.5
C13—C14—H14	119.8	C26—C27—H27C	109.5
C15—C14—H14	119.8	H27A—C27—H27C	109.5
C16—C15—C14	119.3(4)	H27B—C27—H27C	109.5
C16—C15—H15	120.4		

Table S3. Geometric parameters (Å, º) for 66DMBP·BRA (2:1) **(2)**

Geometric parameters [Å, º] for **(2)**			
bond lengths [Å]			
Br1—C1	1.905(3)	C27—H27A	0.9800
C1—C3	1.398(3)	C27—H27B	0.9800
C1—C2	1.411(3)	C27—H27C	0.9800
C2—O2	1.238(3)	N11—C16	1.346(3)
C2—C3^{i}	1.555(3)	N11—C12	1.351(3)
C3—O3	1.250(3)	N11—H11	0.87(3)
C3—C2^{i}	1.555(3)	C12—C13	1.387(3)
N21—C22	1.341(3)	C13—C14	1.381(3)
N21—C26	1.342(3)	C13—H13	0.9500
C22—C23	1.393(3)	C14—C15	1.386(3)
C22—C12	1.483(3)	C14—H14	0.9500
C23—C24	1.383(3)	C15—C16	1.390(3)
C23—H23	0.9500	C15—H15	0.9500
C24—C25	1.383(3)	C16—C17	1.497(3)
C24—H24	0.9500	C17—H17A	0.9800
C25—C26	1.394(3)	C17—H17B	0.9800
C25—H25	0.9500	C17—H17C	0.9800
C26—C27	1.505(3)		
angles [º]			
C3—C1—C2	124.0(2)	C26—C27—H27C	109.5
C3—C1—Br1	117.86(18)	H27A—C27—H27C	109.5
C2—C1—Br1	117.99(17)	H27B—C27—H27C	109.5
O2—C2—C1	125.9(2)	C16—N11—C12	123.5(2)
O2—C2—C3^{i}	116.3(2)	C16—N11—H11	117.9(17)
C1—C2—C3^{i}	117.9(2)	C12—N11—H11	118.4(17)
O3—C3—C1	125.8(2)	N11—C12—C13	118.8(2)
O3—C3—C2^{i}	116.1(2)	N11—C12—C22	119.3(2)
C1—C3—C2^{i}	118.1(2)	C13—C12—C22	121.9(2)
C22—N21—C26	118.1(2)	C14—C13—C12	119.3(2)
N21—C22—C23	123.8(2)	C14—C13—H13	120.3
N21—C22—C12	114.2(2)	C12—C13—H13	120.3
C23—C22—C12	121.9(2)	C13—C14—C15	120.4(2)
C24—C23—C22	117.5(2)	C13—C14—H14	119.8
C24—C23—H23	121.3	C15—C14—H14	119.8
C22—C23—H23	121.3	C14—C15—C16	119.2(2)
C23—C24—C25	119.5(2)	C14—C15—H15	120.4
C23—C24—H24	120.3	C16—C15—H15	120.4
C25—C24—H24	120.3	N11—C16—C15	118.8(2)

C24—C25—C26	119.4(2)	N11—C16—C17	117.4(2)
C24—C25—H25	120.3	C15—C16—C17	123.8(2)
C26—C25—H25	120.3	C16—C17—H17A	109.5
N21—C26—C25	121.7(2)	C16—C17—H17B	109.5
N21—C26—C27	116.5(2)	H17A—C17—H17B	109.5
C25—C26—C27	121.7(2)	C16—C17—H17C	109.5
C26—C27—H27A	109.5	H17A—C17—H17C	109.5
C26—C27—H27B	109.5	H17B—C17—H17C	109.5
H27A—C27—H27B	109.5		

Symmetry code: (i) $-x+1$, $-y$, $-z+2$.

Table S4. Geometric parameters (Å, º) for 66DMBP·IA (1:1) **(3)**

Geometric parameters [Å, º] for **(3)**			
bond lengths [Å]			
I1A—C1A	2.093(3)	C14—C15	1.388(4)
C1A—C2A	1.402(4)	C14—H14	0.9500
C1A—C3A	1.403(4)	C15—C16	1.391(4)
O2A—C2A	1.243(3)	C15—H15	0.9500
C2A—C3A^{i}	1.569(3)	C16—C17	1.498(4)
O3A—C3A	1.242(3)	C17—H17A	0.9800
C3A—C2A^{i}	1.569(3)	C17—H17B	0.9800
I1B—C1B	2.083(3)	C17—H17C	0.9800
C1B—C3B	1.347(4)	N21—C26	1.332(3)
C1B—C2B	1.463(4)	N21—C22	1.357(3)
O2B—C2B	1.215(3)	C22—C23	1.388(4)
C2B—C3B^{ii}	1.525(4)	C23—C24	1.385(4)
O3B—C3B	1.327(3)	C23—H23	0.9500
O3B—H3B	0.9000	C24—C25	1.378(4)
C3B—C2B^{ii}	1.525(4)	C24—H24	0.9500
N11—C16	1.345(3)	C25—C26	1.402(4)
N11—C12	1.366(3)	C25—H25	0.9500
N11—H11	0.9000	C26—C27	1.505(4)
C12—C13	1.388(4)	C27—H27A	0.9800
C12—C22	1.478(4)	C27—H27B	0.9800
C13—C14	1.376(4)	C27—H27C	0.9800
C13—H13	0.9500		
angles [º]			
C2A—C1A—C3A	122.9(2)	C16—C15—H15	120.5
C2A—C1A—I1A	118.20(18)	N11—C16—C15	119.0(2)
C3A—C1A—I1A	118.61(18)	N11—C16—C17	117.7(2)
O2A—C2A—C1A	127.1(2)	C15—C16—C17	123.3(2)
O2A—C2A—C3A^{i}	114.8(2)	C16—C17—H17A	109.5
C1A—C2A—C3A^{i}	118.1(2)	C16—C17—H17B	109.5
O3A—C3A—C1A	125.9(2)	H17A—C17—H17B	109.5
O3A—C3A—C2A^{i}	115.7(2)	C16—C17—H17C	109.5
C1A—C3A—C2A^{i}	118.4(2)	H17A—C17—H17C	109.5
C3B—C1B—C2B	120.1(2)	H17B—C17—H17C	109.5
C3B—C1B—I1B	121.68(19)	C26—N21—C22	118.1(2)
C2B—C1B—I1B	118.09(19)	N21—C22—C23	123.0(2)
O2B—C2B—C1B	124.1(2)	N21—C22—C12	113.4(2)
O2B—C2B—C3B^{ii}	117.8(2)	C23—C22—C12	123.5(2)
C1B—C2B—C3B^{ii}	118.1(2)	C24—C23—C22	118.1(2)

C3B—O3B—H3B	111.6	C24—C23—H23	120.9
O3B—C3B—C1B	122.9(2)	C22—C23—H23	120.9
O3B—C3B—C2B^{ii}	115.5(2)	C25—C24—C23	119.3(3)
C1B—C3B—C2B^{ii}	121.6(2)	C25—C24—H24	120.3
C16—N11—C12	123.6(2)	C23—C24—H24	120.3
C16—N11—H11	114.2	C24—C25—C26	119.2(3)
C12—N11—H11	122.1	C24—C25—H25	120.4
N11—C12—C13	117.8(2)	C26—C25—H25	120.4
N11—C12—C22	119.5(2)	N21—C26—C25	122.0(2)
C13—C12—C22	122.7(2)	N21—C26—C27	116.7(2)
C14—C13—C12	120.2(2)	C25—C26—C27	121.3(2)
C14—C13—H13	119.9	C26—C27—H27A	109.5
C12—C13—H13	119.9	C26—C27—H27B	109.5
C13—C14—C15	120.4(2)	H27A—C27—H27B	109.5
C13—C14—H14	119.8	C26—C27—H27C	109.5
C15—C14—H14	119.8	H27A—C27—H27C	109.5
C14—C15—C16	119.1(2)	H27B—C27—H27C	109.5
C14—C15—H15	120.5		

Symmetry codes: (i) -x+1, -y+1, -z+1; (ii) -x+2, -y+1, -z+2.

Table S5. Hydrogen-bond geometry and π···π interaction geometries [Å, º] for **1**, **2** and **3**.

a)

66DMBP·BRA **(1)**				
D—H···*A*	*D*—H	H···*A*	*D*···*A*	*D*—H···*A*
O2—H2···N21	0.99(4)	1.76(4)	2.698(4)	157(4)
N11—H11···O3	1.04(4)	1.65(4)	2.678(4)	169(3)
C13—H13···O6^{i}	0.95	2.49	3.428(4)	171
C15—H15···Br2^{ii}	0.95	2.80	3.609(4)	143
C17—H17*A*···O5^{iii}	0.98	2.38	3.239(5)	146
C23—H23···O5^{i}	0.95	2.46	3.367(4)	159
C23—H23···O6^{i}	0.95	2.54	3.272(5)	134
C25—H25···Br1^{iv}	0.95	2.89	3.835(5)	178
C27—H27*A*···O6^{v}	0.98	2.46	3.425(5)	169

Symmetry codes: (i) *x*, *y*+1, *z*; (ii) -*x*+1, *y*+1/2, -*z*+3/2; (iii) *x*, -*y*+1/2, *z*+1/2; (iv) -*x*, *y*+1/2, -*z*+1/2; (v) *x*, -*y*+1/2, *z*-1/2.

C(X)	*C(Y)*	*C(X)···C(Y)*	*Dihedral angle*	*C(X)$_{perp}$*
C(1)	C(2)^{i}	3.752(3)	6.040(5)	3.527(4)

C(1) and C(2)^{i} are centroids of N11/C12/C13/C14/C15/C16 and N21/C22/C23/C24/C25/C26 rings, respectively. C(X)$_{perp}$ is the perpendicular distance of C(X) on plane Y. Symmetry code: (i) *x*, -*y*+1/2, *z*+1/2.

b)

66DMBP·BRA (2:1) **(2)**				
D—H···*A*	*D*—H	H···*A*	*D*···*A*	*D*—H···*A*
N11—H11···O2^{i}	0.87(3)	2.48(3)	3.099(3)	129(2)
N11—H11···O3	0.87(3)	1.85(3)	2.665(3)	155(2)
C17—H17*B*···Br1^{ii}	0.98	2.98	3.895(3)	156
C23—H23···O2^{i}	0.95	2.58	3.500(3)	164
C25—H25···Br1^{iii}	0.95	3.10	3.973(3)	153
C13—H13···Br1^{iv}	0.95	3.09	4.002(3)	161
C15—H15···Br1^{ii}	0.95	3.14	3.934(3)	143
C15—H15···O3^{ii}	0.95	2.62	3.481(3)	151

Symmetry codes: (i) -*x*+1, -*y*, -*z*+2; (ii) *x*-1, *y*, *z*; (iii) *x*, *y*, *z*-1; (iv) *x*-1, *y*, *z*-1.

c)

66DMBP·IA (2:1:1) **(3)**				
D—H···*A*	*D*—H	H···*A*	*D*···*A*	*D*—H···*A*
N11—H11···O3*A*	0.90	1.95	2.791(3)	155
N11—H11···O2*A*^{ii}	0.90	2.28	2.925(3)	128
O3*B*—H3*B*···O2*A*	0.90	1.90	2.657(3)	140
C15—H15···I1*A*^{i}	0.95	3.14	4.074(3)	168
C17—H17*A*···O2*A*^{ii}	0.98	2.56	3.228 (3)	125
C27—H27*C*···I1*A*^{iv}	0.98	3.25	4.039 (3)	139
C23—H23···O3*A*	0.95	2.52	3.155(3)	125

Symmetry codes: (i) *x*, *y*, *z*-1; (ii) -*x*+1, -*y*+1, -*z*+1; (iii) -*x*+2, -*y*+1, -*z*+2; (v) -*x*, -*y*, -*z*+1.

C(X)	*C(Y)*	*C(X)···C(Y)*	*Dihedral angle*	*C(X)$_{perp}$*
C(1)	C(2)	3.561(2)	1.452(2)	3.402(3)
C(2)	C(3)	3.675(2)	0	3.388(4)

C(1), C(2) and C(3) are centroids of C1B/C2B/C3B^{i}/C1B^{i}/C2B^{i}/C3B, N11^{ii}/C12^{ii}/C13^{ii}/C14^{ii}/C15^{ii}/C16^{ii} and N11^{iii}/C12^{iii}/C13^{iii}/C14^{iii}/C15^{iii}/C16^{iii} rings, respectively. C(X)$_{perp}$ is the perpendicular distance of C(X) on plane Y. Symmetry code: (i) -*x*+2, -*y*+1, -*z*+2; (ii) -*x*+1, -*y*+1, -*z*+1; (iii) *x*+1, *y*+1, *z*+1.

a) pure 66DMBP

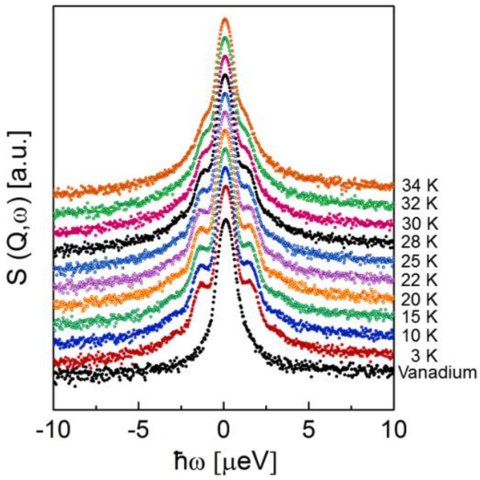

b) 66DMBP·BRA (2:1) **(2)**

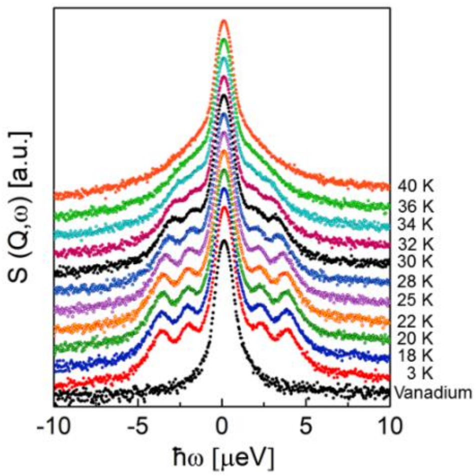

c) 66DMBP·IA **(3)**

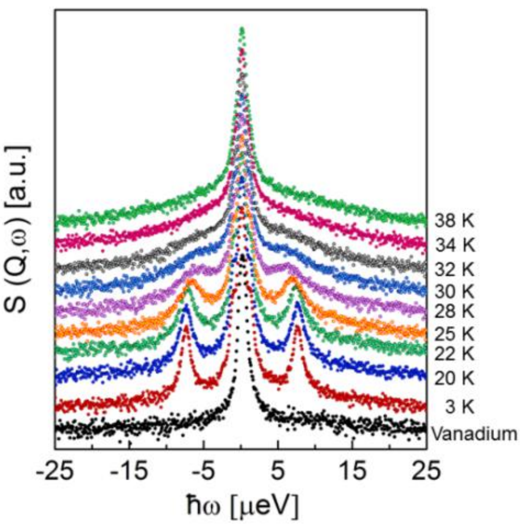

Fig. S5. Tunneling results at several temperatures in the energy range between ±10 and ±25 μeV for **1**, **2**, and **3** respectively.

a) pure 66DMBP

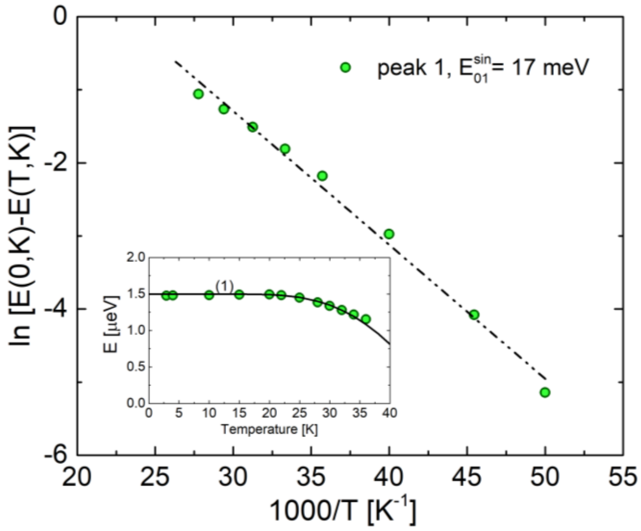

b) 66DMBP·BRA (2:1) **(2)**

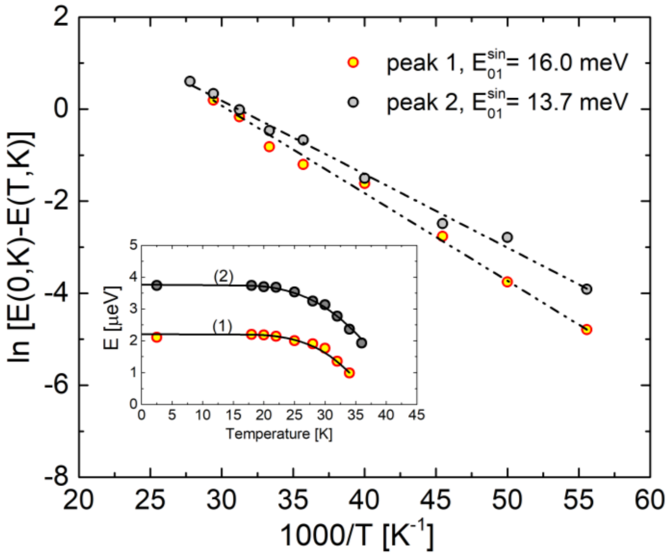

c) 66DMBP·IA **(3)**

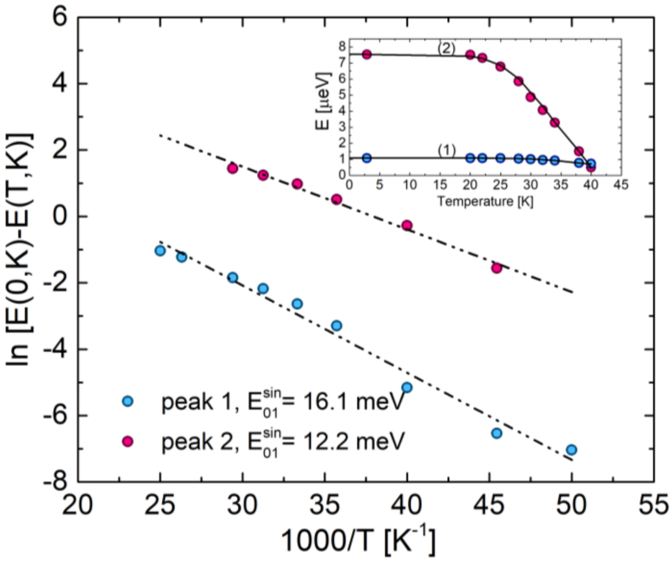

Fig. S6. Arrhenius plots for the energy of excitation between librational energy levels, E_{01}^{sin} calculated for **1**, **2**, **3** complexes. Inset: the temperature dependencies for the peak positions.

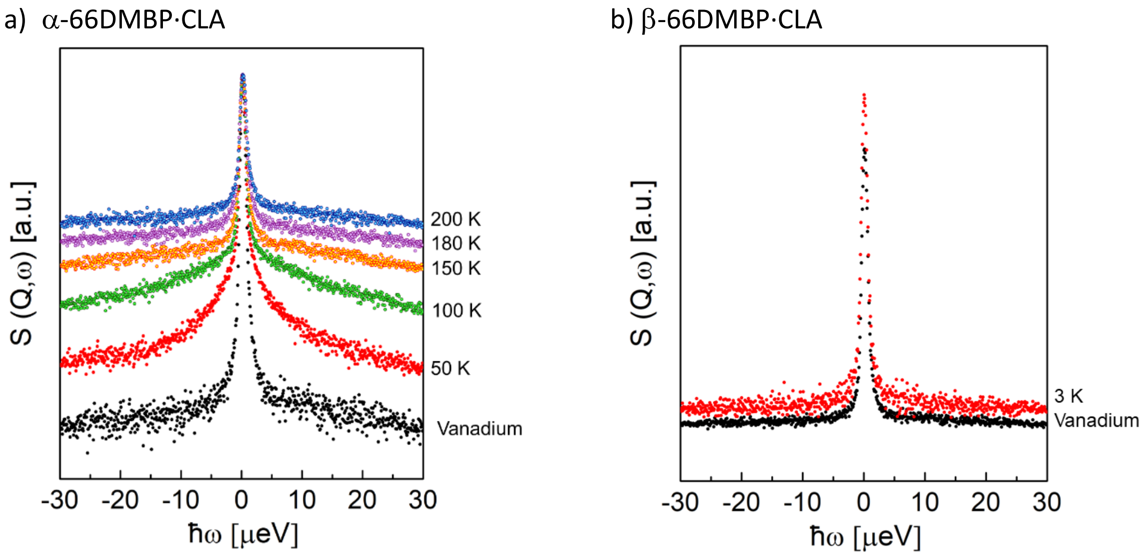

Fig. S7. QENS signals measured for a) α-66DMBP·CLA for integrated Q range. b) Tunneling spectra for β-66DMBP·CLA at several temperatures in the energy range between ±10 and ±25 μeV for **1**, **2**, and **3,** respectively.

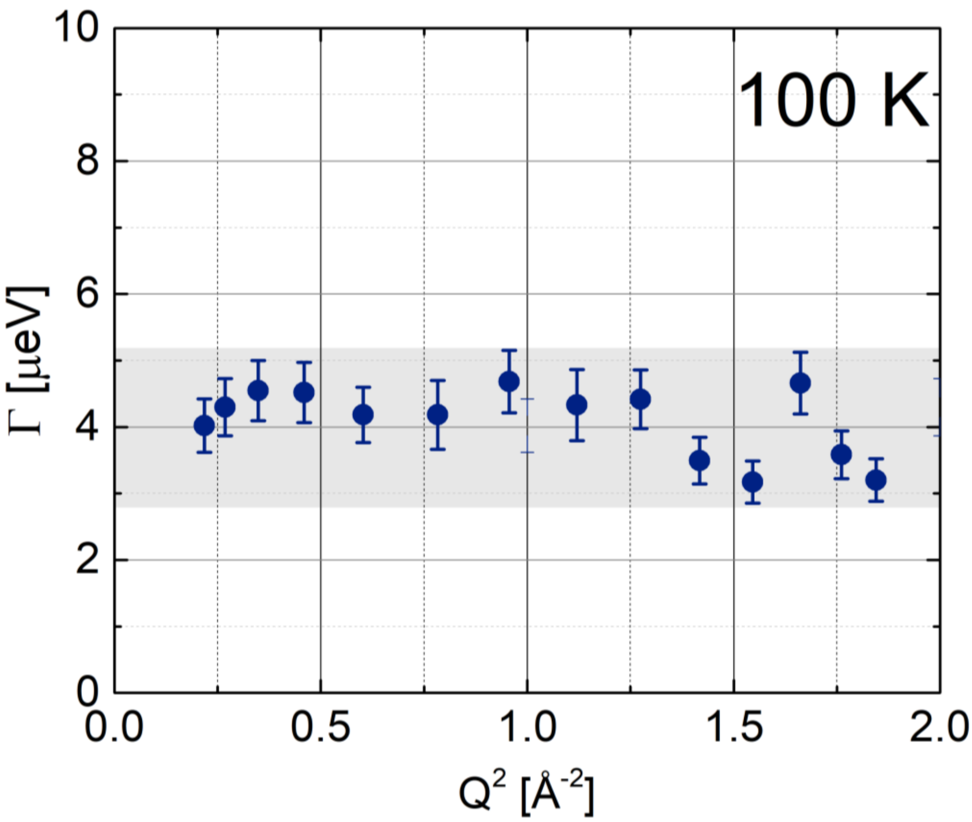

Fig. S8. Q-dependence of Γ estimated from the fitting to the data taken on SPHERES spectrometer.